Spontaneous, pH-Dependent Membrane Insertion of a Transbilayer α-Helix†

John F. Hunt,‡,|| Parshuram Rath,§ Kenneth J. Rothschild,§ and Donald M. Engelman*,‡

Department of Molecular Biophysics and Biochemistry, Yale University, New Haven, Connecticut 06511, and Department of Physics and Molecular Biophysics Laboratory, Boston University, Boston, Massachusetts 02215

Received January 23, 1997; Revised Manuscript Received September 3, 1997⊗

ABSTRACT: A question of fundamental importance concerning the biosynthesis of integral membrane proteins is whether transmembrane secondary structure can insert spontaneously into a lipid bilayer. It has proven to be difficult to address this issue experimentally because of the poor solubility in aqueous solution of peptides and proteins containing these extremely hydrophobic sequences. We have identified a system in which the kinetics and thermodynamics of α-helix insertion into lipid bilayers can be studied systematically and quantitatively using simple spectroscopic assays. Specifically, we have discovered that a 36-residue polypeptide containing the sequence of the C-helix of the integral membrane protein bacteriorhodopsin exhibits significant solubility in aqueous buffers free of both detergents and denaturants. This helix contains two aspartic acid residues in the membrane-spanning region. At neutral pH, the peptide associates with lipid bilayers in a nonhelical and presumably peripheral conformation. With a pK_a of 6.0, the peptide inserts into the bilayer as a transbilayer α-helix. The insertion reaction proceeds rapidly at room temperature and is fully reversible.

Biochemists and cell biologists have debated the relative contributions of spontaneous membrane insertion and catalyzed membrane insertion to the assembly of integral membrane proteins in living cells (von Heijne & Blomberg, 1979; Wickner, 1980; Engelman & Steitz, 1981; von Heijne, 1994b). Theoreticians have proposed that the spontaneous insertion of protein secondary structure into the membrane could be driven by the large release of free energy associated with the partitioning of a hydrophobic polypeptide from aqueous solution into a phospholipid bilayer if the energy barrier for the insertion event is not too high (von Heijne & Blomberg, 1979; Engelman & Steitz, 1981). However, extensive research on the mechanism of protein secretion has led to the identification of enzymes involved in the translocation of soluble proteins across biological membranes (Nicchitta et al., 1991; Bassford et al., 1991), and cell biologists have proposed that these same enzymes could catalyze the insertion of protein secondary structure into the membrane (Blobel, 1980; Anderson et al., 1983; Audigier et al., 1987).

The membrane-spanning α-helix plays a central role in this debate. Theoreticians have observed that this structure should be an energetically favorable conformation for a hydrophobic polypeptide sequence of adequate length because it systematically satisfies the hydrogen bonding requirements of the polypeptide backbone while simultaneously burying the hydrophobic side-chains in the hydrophobic core of the phospholipid bilayer (von Heijne & Blomberg, 1979; Engelman & Steitz, 1981). This idea has been exploited in the development of sequence analysis algorithms for the prediction of the location of membrane-spanning α-helices in integral membrane proteins (von Heijne, 1980; Kyte & Doolittle, 1982; Engelman et al., 1986). These algorithms are believed to be quite reliable (Engelman et al., 1986), although the structures of relatively few α-helical integral membrane proteins have been characterized at an adequate level of resolution to provide a rigorous test.

One such algorithm calculates the free energy change expected for the partitioning of a random coil in aqueous solution into a phospholipid bilayer in the form of a transbilayer α-helix (Engelman & Steitz, 1981). For an adequately hydrophobic sequence, the free energy released in the course of such a partitioning reaction is thought to be quite large. For the experimentally observed transbilayer α-helices, the energies have been calculated at 16−40 kcal/mol or approximately 26−65 times *kT* at physiological temperature (Engelman et al., 1986), although the actual free energy of insertion has proven to be difficult to evaluate experimentally (Leto & Holloway, 1979; Moll & Thompson, 1994; Ben-Efraim et al., 1994; Soekarjo et al., 1996). This release of energy could drive the spontaneous membrane insertion of transbilayer α-helices in the course of integral membrane protein biosynthesis (von Heijne & Blomberg, 1979; Wickner, 1980; Engelman & Steitz, 1981).

However, a troubling ambiguity in all of these theoretical schemes concerns the kinetics of the insertion process. Irrespective of the equilibrium driving energy in a chemical reaction, the rate of the reaction is determined by the energy barriers which have to be crossed along the reaction pathway. A large energy barrier exists for transbilayer α-helix insertion because of the necessity of translocating polar groups and electrostatic charge through the hydrophobic core of the bilayer in the course of the reaction. The termini of an α-helix are strongly polar, and the sequences flanking transmembrane helices often contain a high density of electrostatic charge (von Heijne & Gavel, 1988; von Heijne, 1994b). There are no reliable estimates for the magnitude of this activation energy barrier, and experimental investiga-

† This work was supported by grants from the NIH (GM22778) and the NSF (MCB9406983) to D.M.E. and grants from the NIH-NEI (EY05499) and the NSF (MCB9419059) to K.J.R.

* Corresponding author.

‡ Yale University.

§ Boston University.

|| Present Address: Department of Biological Sciences, Columbia University, New York, NY 10027. E-mail: hunt@sid.bio.columbia.edu.

⊗ Abstract published in *Advance ACS Abstracts,* November 1, 1997.

S0006-2960(97)00147-5 CCC: $14.00

tion of the process has proven difficult because of the poor solubility in aqueous solution of polypeptides containing the extremely hydrophobic sequences found in transbilayer α-helices (Leto & Holloway, 1979; Moll & Thompson, 1994; Ben-Efraim et al., 1994; Soekarjo et al., 1996; Chung & Thompson, 1996).

In spite of this complication, there have been many experimental investigations of integral membrane protein assembly, using biochemical (Enoch et al., 1979; Silver et al., 1981; Watts et al., 1981; Geller & Wickner, 1985; Surrey et al., 1996; Anderson et al., 1983; Mueckler & Lodish, 1986; Audigier et al., 1987; Bayle et al., 1995; Denzer et al., 1995) and biophysical (Slatin et al., 1994; Soekarjo et al., 1996; Peled & Shai, 1994; Goormaghtigh et al., 1991; McKnight et al., 1991; de Kruijff, 1994; Popot et al., 1987; Booth et al., 1996) techniques *in vitro* as well as genetic techniques *in vivo* in bacteria (Wolfe et al., 1985; McGovern & Beckwith, 1991; Manoil & Beckwith, 1986; Andersson & von Heijne, 1993; Whitley et al., 1994; Cao et al., 1995; Traxler & Murphy, 1996; von Heijne, 1989, 1994b). These studies have come to differing conclusions, although many of them have suggested that spontaneous insertion of transbilayer α-helices may occur on a physiologically relevant time scale (Watts et al., 1981; Geller & Wickner, 1985; Surrey et al., 1996; Abrams et al., 1991; Slatin et al., 1994). For example, many protein toxins seem to be capable of spontaneously inserting into pure phospholipid membranes (Abrams et al., 1991; Slatin et al., 1994; Miczak et al., 1996; Neville & Hudson, 1986). Also, *in vivo* physiological experiments have shown that polypeptide segments shorter than 60 residues in length that are attached to transmembrane α-helices can be translocated across the cytoplasmic membrane of *Escherichia coli* without the involvement (Andersson & von Heijne, 1993; von Heijne, 1994a,b) of the well-characterized secretory machinery encoded by the *sec* genes (Bassford et al., 1991). Therefore, under these circumstances, the membrane insertion process might proceed spontaneously and without catalysis *in vivo*. However, the accepted interpretation of these physiological experiments has recently been challenged (Traxler & Murphy, 1996).

Biophysical data on the process of integral membrane protein insertion into bilayers would be useful in establishing fundamental structural and thermodynamic principles which could help guide the resolution of controversies of this kind. Unfortunately, the experimental systems developed to date have not allowed direct evaluation of either the kinetics or the sequence dependence of the membrane insertion reaction, and even the equilibrium thermodynamics of this process have proven to be difficult to characterize in detail (Leto & Holloway, 1979; Moll & Thompson, 1994; Ben-Efraim et al., 1994; Peled & Shai, 1994; Reddy et al., 1994; Soekarjo et al., 1996; Peled-Zehavi et al., 1996; Chung & Thompson, 1996). In summary, in the absence of a direct kinetic assay for the integration of α-helices into lipid bilayers, the relative contribution of spontaneous insertion and catalyzed insertion to the assembly of integral membrane proteins remains controversial.

In this paper, we report the identification of a system in which the kinetics and thermodynamics of α-helix integration into lipid bilayers can be assayed directly using simple spectroscopic techniques. We have synthesized a polypeptide based on the sequence of the C-helix in the integral membrane protein bacteriorhodopsin (BR)[1] (Oesterhelt & Stoeckenius, 1971; Henderson et al., 1990; Khorana, 1988), which functions as a light-driven proton pump. The peptide comprises residues 72 through 107 in the sequence of mature BR with the substitution of a glutamic acid for the glutamine at position 105 in the second cytoplasmic loop of the native protein. The sequence of the BR-C peptide is shown schematically in Figure 1. It contains two aspartic acid residues in the putative membrane-spanning region (Grigorieff et al., 1996; Engelman et al., 1986), allowing the overall hydrophobicity of the sequence to be modulated by pH. In native BR, these two residues play a key role in proton transport with asp-85 serving as the proton acceptor and asp-96 serving as the proton donor to the Schiff base (Bousché et al., 1991, 1992; Rothschild & Sonar, 1995). We have discovered that the BR-C peptide exhibits significant solubility at neutral pH in aqueous buffers free of both detergents and chaotropic agents. The favorable solubility properties of this peptide allow its interaction with phospholipid membranes to be studied and assayed in a straightforward manner. Membrane insertion of the peptide is pH dependent (Bechinger, 1996) and occurs rapidly at room temperature.

EXPERIMENTAL PROCEDURES

Peptide Methods. The BR-C peptide was synthesized using *t*-BOC chemistry by James Elliot at the W. M. Keck Foundation Biotechnology Resource Laboratory at Yale University; it was purified by reversed phase chromatography on a C18 phase using a water/acetonitrile/TFA gradient. In a typical preparation of the soluble form of the peptide, the lyophilized powder was dissolved at approximately 0.5 mg/mL in a solution containing 6 M urea, 200 mM NaCl, 10 mM Tris, pH 8.3. The peptide solution was dialyzed twice against 300 vol of the same buffer without urea and then dialyzed three times against 300 vol of 20 mM NaCl, 5 mM $NaPO_4$, pH 8.0. The total time in dialysis was always in excess of 30 h with a minimum of 3 h for each of the five buffer changes. Following removal from dialysis, the solution was passed through a 0.22 μm polycarbonate syringe filter (CoStar, Cambridge, MA) yielding a final peptide concentration greater than 350 μg/mL based on quantitative amino acid analysis. The concentration of residual urea was estimated to be in the picomolar range.

Phospholipid Methods. Synthetic dimyristoylphosphatidylcholine (DMPC) was purchased from Avanti (Highbluff, AL). The polar lipid extract from *Halobacterium salinarium* was prepared according to the method of Kates et al. (1982). Phospholipid vesicles were prepared as follows: The phospholipid was dissolved in $CHCl_3$, and a trace amount of ^{14}C-labeled dipalmitoylphosphatidylcholine was added to allow facile monitoring of the lipid concentration. Following removal of the solvent using a rotary evaporator, the phospholipid film was dried at high vacuum (<100 millitorr) overnight and then rehydrated at 20 mg/mL in water. The suspension was sonicated in a bath sonicator at approximately 50 °C for 60 min and then frozen at −20 °C. Prior to each experiment, an aliquot of this stock solution was treated with 6 bursts form a microtip probe sonicator (10 s each). The

[1] Abbreviations: BR, bacteriorhodopsin; CD, circular dichroism; FTIR, Fourier transform infrared spectroscopy; *Halo*-lipids, *Halobacterium salinarium* polar lipids.

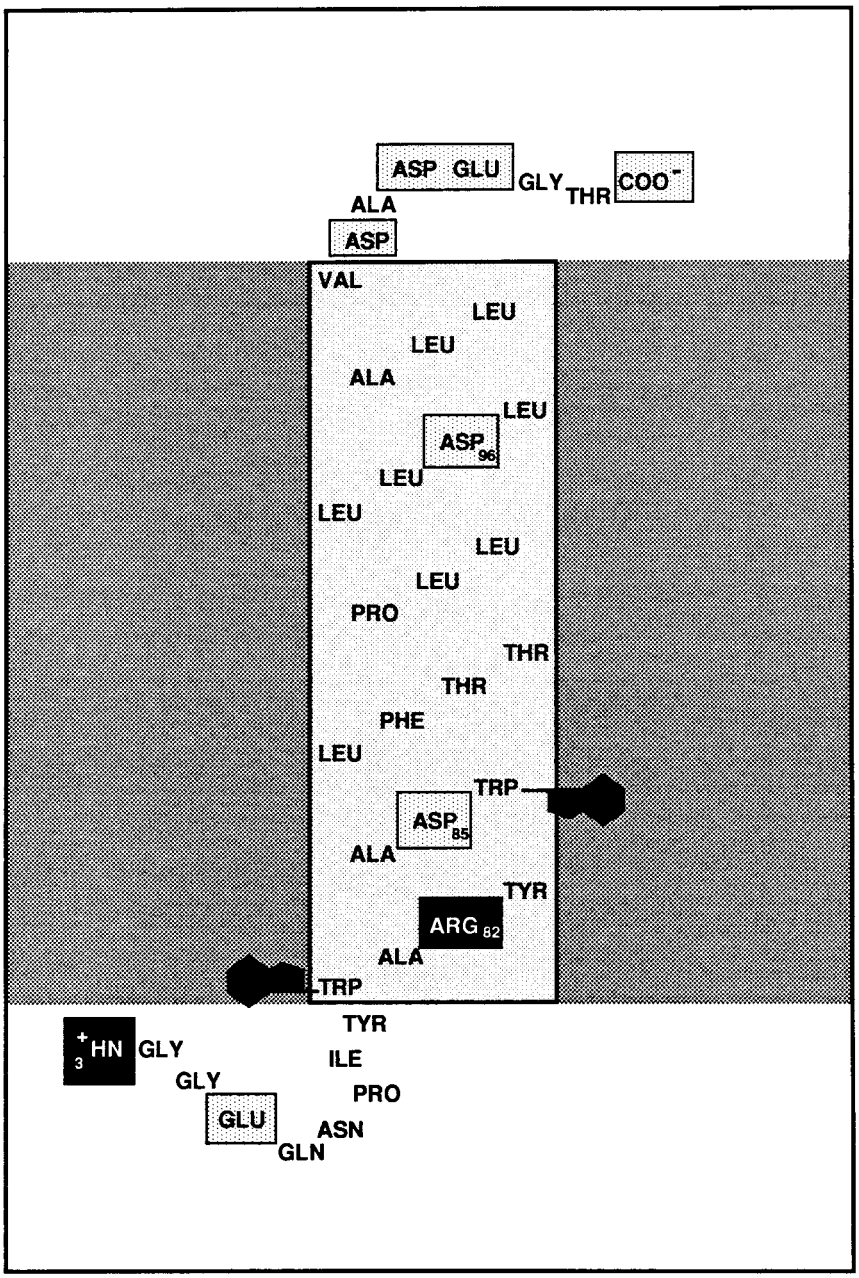

FIGURE 1: Schematic diagram of the synthetic BR-C peptide used in our studies. This sequence corresponds to the third transmembrane helix in the integral membrane protein bacteriorhodopsin (BR). The peptide comprises residues 72−107 in the primary structure of mature BR except for the substitution of a glutamic acid for the glutamine at position 105 in the second cytoplasmic loop of the native protein. The dark gray areas in the diagram represent the location of the lipid bilayer relative to this section of the protein sequence in the native tertiary structure of BR as inferred by Henderson et al. (1990) using high-resolution electron crystallography.

vesicles were then passed through a 0.45 μm polycarbonate centrifugal filter (CoStar); the yield of phospholipid during filtration was greater than 95%. The DMPC vesicles were stored at 35 °C pending use; the *Halo*-lipid vesicles were handled at 25 °C.

Preparation and Manipulation of Protein/Phospholipid Multilayers. The soluble BR-C peptide stock was diluted to 37 μg/mL and incubated at room temperature for 8 h. DMPC vesicles were added to a final concentration of 330 μg/mL, and incubation was continued overnight. The sample was placed under vacuum, and its volume was reduced by a factor of 6 prior to dialysis into a buffer containing 3 μM NaCl, 350 μM NaH_2PO_4, pH $\approx$ 5.8 (for approximately 24 h at room temperature). Finally, the sample was sonicated 6 times with 10 s bursts from a microtip probe sonicator, filtered through a 0.22 μm polycarbonate syringe filter, and stored at −20 °C pending use. Immediately prior to deposition, the sample was thawed and titrated to the indicated pH using either HCl or NaOH.

Films were deposited on AgCl windows (Fisher, Plainfield, NJ) using isopotential spin-dry centrifugation (Clark et al., 1980), a technique which involves gradual dehydration of the sample while it is held in a centrifugal field in an ultracentrifuge rotor. Centrifugation proceeded for at least 6 h at 22 °C. Each multilamellar film nominally contained 160 μg of the BR-C peptide and 1.5 mg of lipid. Following deposition, the windows were transferred to a sealed sample holder where the films were rehydrated by vapor diffusion in an atmosphere maintained at 98% relative humidity by a saturated solution of K_2SO_4 in water. Rehydration was allowed to proceed for a minimum of 12 h at room temperature. For the sample in DMPC, acidification *in situ* was effected by adding 6.5 μL of 0.1 N HCl directly to the surface of the film; bulk water was allowed to evaporate in

room air before the film was returned to the sample chamber in order to re-equilibrate at 98% relative humidity. An equivalent protocol was used for the preparation of samples in *Halo*-lipids except that the *Halo*-lipid multilayers were deposited at pH 8.2 from 800 μL of a buffer containing 1.3 mM NaCl, 330 μM $NaHPO_4$ and were acidified *in situ* with 600 nmol of HCl.

HPLC Gel Filtration Chromatography. An aliquot of the soluble BR-C peptide was dialyzed into 20 mM NaCl, 5 mM $NaPO_4$, pH 6.0 and then concentrated to greater than 1 mg/mL using a Centricon (Amicon, Dover, MA). A 125 μL sample of the peptide was injected onto a TSK SW2000 silica-based gel filtration column (Bio-Rad, Richmond, CA) equilibrated in 200 mM NaCl, 50 mM $NaPO_4$, 0.025% (w/v) NaN_3, pH 6.2. The column was eluted at room temperature with a solvent flow rate of 0.5 mL/min, and the optical density of the column effluent was monitored at 280 nm. Fractions were stored at 4 °C between runs. Bovine thyroglobulin (670 kDa) was used as a marker for the void volume while vitamin B12 (1.35 kDa) was used as a marker for the fully included volume; the column was calibrated by fitting a straight line to a plot of $\ln(R_s)$ against K_{av} (le Maire et al., 1989) for chicken ovalbumin (44 kDa; $R_s = 28$ Å) and horse myoglobin (17 kDa; $R_s = 19$ Å) (le Maire et al., 1986).

Titration Experiments in Phospholipid Vesicles in Solution. All experiments were conducted in a buffer containing 20 mM NaCl and 5 mM $NaPO_4$. NaOH and HCl were used to adjust the pH of the peptide sample, which was measured using a microelectrode (Microelectrodes Inc., Manchester, NH). For the fluorescence experiments, the pH was monitored directly in the fluorescence cuvette. Experiments using DMPC vesicles were conducted at 35 °C (*i.e.* well above the phospholipid phase transition temperature), while experiments using *Halo*-lipid vesicles were conducted at 25 °C. Before the initiation of any spectroscopic experiment, a stock solution of the soluble BR-C peptide at approximately 360 μg/mL was diluted to a final concentration of approximately 12 μg/mL (at pH 7.8) and incubated for a minimum of 8 h at the appropriate temperature for the experiment. In both phospholipid and pH titration experiments, successive additions were spaced a minimum of 15 min apart. The pH titrations of the peptide were conducted in the presence of 250 μg/mL DMPC or 300 μg/mL *Halo*-lipid.

Fluorescence Spectroscopy. Fluorescence data were acquired using an SLM8000 spectrofluorometer with all slits set to 4 nm. For both binding and pH titration experiments in DMPC, the intrinsic fluorescence of the BR-C peptide was monitored at 328 nm. Binding to *Halo*-lipid vesicles was monitored by the quenching of the intrinsic fluorescence of the peptide at 360 nm; we believe that this quenching is attributable to resonance energy transfer to contaminating fluorophores in the lipid preparation since there is a peak at 355 nm in the fluorescence excitation spectrum of pure *Halo*-lipid vesicles (when monitored at an emission wavelength of 430 nm).

Curve Fitting and Parameter Estimation. Nonlinear curve fitting of the fluorescence binding data in DMPC was accomplished using the Marqurdt−Levenberg algorithm as implemented in the commercially available program PeakFit (Jandel Scientific, Cotati, CA). The functional form of the binding curve was assumed to be $F([\text{DMPC}]) = F_o + \Delta F \phi_b[\text{DMPC}]$, where F_o represents the fluorescence of the unbound peptide, ΔF represents the change in fluorescence upon binding, and ϕ_b represents the fraction of peptide bound at a given concentration of phospholipid as described by the function specified at the relevant point in the Results section; four parameters were optimized, *i.e.* F_o, ΔF, K_d, and n. The binding curve for *Halo*-lipids was analyzed using a simple two-state model, *i.e.* $F([\text{lipid}]) = F_o + \Delta F([\text{lipid}]/(K_d + [\text{lipid}]))$; this equation is appropriate because the values of $(K_d/[\text{BR-C}])$ were very large (>100) in these assays. The size of the binding site, n, cannot be determined in this regime of (K_d/n), so $n = 9$ was assumed in estimating the binding energy. The dissociation constant for *Halo*-lipids was evaluated by nonlinear curve-fitting of the fluorescence binding data as well as by linear regression to the data in double-reciprocal format.

CD Spectroscopy. Protein concentrations were verified at the end of each assay by quantitative amino acid analysis, and these values were used to normalize the mean residue ellipticity. CD spectra were acquired using an Aviv 60DS spectropolarimeter. Samples were measured in a 1.00 cm path length jacketed cuvette. Raw data were acquired at a 0.5 nm interval using a 2.0 s averaging time, and at least three such scans were averaged for each sample. Protein spectra were processed as follows: An appropriate background spectrum (*i.e.* buffer with or without lipid) was subtracted from the raw data. Next, the average value of the ellipticity in the difference spectrum was computed in the wavelength range from 265 to 290 nm, and this small offset (<0.8 millidegrees) was subtracted from every point in the spectrum. Finally, the spectrum was smoothed using the method of Savitsky and Golay (1964) with a third-order polynomial applied in a window of 13 points (±3 nm). For the CD data presented in Table 1, the mean residue ellipticity of the membrane-bound form of the BR-C peptide at pH 8 was calculated by correcting the observed ellipticity for the fraction of the peptide bound to the vesicles at the operative phospholipid concentration (using the dissociation constants estimated from the fluorescence binding experiments and listed in column 1 of Table 1). It was assumed that 100% of the peptide was bound to the vesicles at pH 4.

Quantitative Analysis of pH Titration Data. The CD data in Figure 4B were used to calculate the pH-dependence of the ratio of the protonated to the deprotonated form of the BR-C peptide in DMPC vesicles (*i.e.* the equilibrium constant for the transition) which is plotted explicitly in Figure 4C. The baseline variations in the CD of the two forms of the peptide were calculated by linear regressions to the four points at the highest pH values and the three points at the lowest pH values (gray lines in Figure 4B). The equilibrium constant for the conformational transition is equal to the ratio of the distance of each data point in Figure 4B from these two baselines. To determine the pK_a of the proton involved in the transition, it is necessary to compensate for the fact that the initial binding reaction is only partially completed under the conditions of the pH titration experiment. If we assume that the reaction mechanism involves one free deprotonated species, one peripherally-bound deprotonated species, and one membrane-inserted protonated species (see the section entitled "The pH-Dependent Transition in DMPC Vesicles" in the Results), the equilibrium can be described mathematically as follows:

$$\log([\text{BR-C}\cdot\text{H}_{\text{inserted}}]/([\text{BR-C}^-_{\text{free}}] + [\text{BR-C}^-_{\text{peripheral}}])) = pK_a^{\text{apparent}} - \log(1 + (K_d/[\text{DMPC}])) - \text{pH}$$

Table 1: Comparison of the Structural Properties of the BR-C Peptide in Different Phospholipid Environments[a]

	K_d for peptide binding to vesicles at pH 7.8 (μg/mL)	θ_{222} for vesicle-bound peptide: at pH8 (deg·cm^2 per dmol·res)	θ_{222} for vesicle-bound peptide: at pH4 (deg·cm^2 per dmol·res)	pK_a of conformational transition in vesicles	no. of proton equivalents titrating during transition in vesicles	peptide backbone orientation in multilayers: at basic pH	peptide backbone orientation in multilayers: after acidification	$\Delta G°_{binding}$ in peripheral conformation (kcal/mol)	$\Delta G_{insertion}$ for protonated peptide (kcal/mol)
DMPC	26 (39 μM)[b]	−6290	−16200	6.03	1.03	isotropic $<P_2>_{A_{II}} = -0.03$[e]	⊥ α-helix $<P_2>_{A_{II}} = -0.23$[e]	-7.5 ± 1.4[h]	−2.9[i]
Halo-lipids	360 (360 μM)[c] 380 (380 μM)[d]	−6210	−15900	6.15	1.02	isotropic $<P_2>_{A_{II}} = -0.02$[f]	⊥ α-helix $<P_2>_{A_{II}} = -0.14$[f,g]	-5.9 ± 1.4[h]	−2.9[i]

[a] The dissociation constants (column 1) were determined by fluorescence emission spectroscopy. CD spectroscopy was used to evaluate the pK_a's (column 4) and the number of protons responsible for the conformational transitions (column 5). The protein amide II order parameters in phospholipid multilayers (columns 6 and 7) were measured using polarized FTIR spectroscopy. [b] Nonlinear curve fitting of fluorescence binding data using complex two-state model ($n = 8.8$); $r^2 = 0.9992$ for 17 points from 0 to 50 μg/mL DMPC. [c] Linear regression to fluorescence binding data in double-reciprocal format; $r^2 = 0.9997$ for 16 points from 20 to 400 μg/mL *Halo*-lipids. [d] Nonlinear curve fitting of fluorescence binding data using simple two-state model; $r^2 = 0.9995$ for 18 points from 0 to 400 μg/mL *Halo*-lipids. [e] Dichroism values determined using automated baseline correction algorithm (see Experimental Procedures). [f] Dichroism values determined by interactive subtraction of parallel and perpendicular spectra. [g] Other samples of the BR-C peptide in *Halo*-lipid vesicles showed an amide II order parameter of approximately −0.18 when deposited directly at acidic pH. [h] Calculated as $\Delta G°_{binding} = RT \ln(K_d/n)$ using the value of K_d in column 1 and assuming that the size of the binding site $n = 9$ phospholipid molecules; the specified limits allow for a 10-fold error in the estimate of (K_d/n). [i] Calculated as $\Delta G°_{insertion} = -RT \ln(10)(pK_a - 4.0)$, *i.e.* assuming a p$K_a$ of 4.0 for the titratable proton in the peripherally-bound conformation of the peptide.

The term K_d in this equation represents the dissociation constant for the binding of the deprotonated peptide to the membrane while the term $K_a^{apparent}$ represents the equilibrium constant for the pH titration of the peripherally-bound peptide and the tightly coupled membrane-insertion reaction. This equation can be applied directly to the analysis of the titration data presented in Figure 4B since the magnitude of the molar ellipticity at 222 nm is very similar for the two deprotonated species.

Polarized FTIR Spectroscopy. During FTIR measurements, the films were sealed into a homemade compression mount to prevent dehydration in the dry environment of the spectrometer (Earnest et al., 1990). FTIR spectra were acquired at ambient temperature at 2 cm^{-1} nominal resolution in a Nicolet 60SX spectrometer equipped with an MCT-B detector and a KRS-5 wire-grid polarizer as described by Earnest et al. (1986). For each sample, absorbance spectra were measured in two polarizations at four different angles of incidence: 0, 38, 45, and 52° inclination of the surface normal of the sample relative to the incident beam (Rothschild & Clark, 1979). A total of 500 interferograms were averaged for all of the spectra except for those acquired at 45° tilt, where 2000 interferograms were averaged.

Dichroism values were evaluated using a fully automated baseline correction and data analysis routine written for the program LabCalc (Galactic Industries, Nashua, NH). The baseline correction algorithm functions as follows: The spectral points at approximately 1800 and 900 cm^{-1} are set to zero using a linear function. Next, the lowest points in each half of the spectral region from 2000 to 700 cm^{-1} are set to zero using a linear function, and this procedure is applied iteratively until the algorithm converges. At a given tilt angle and frequency, the dichroic ratio R is calculated as the ratio of the sample absorbance with the incident beam polarized parallel *vs* perpendicular to the optical plane of incidence (Earnest et al., 1986). Order parameters were calculated as described by Rothschild and Clark (1979), *i.e.* by linear regression to the dichroism data plotted in the form $R = (3<P_2>/(1 - <P_2>))\sin^2(\alpha)$; the refractive index of the protein/lipid film was assumed to be 1.55. The dichroism plots from the tilt series data are shown explicitly in Figure S1 in the Supporting Information.

RESULTS

Preparation of the Soluble BR-C Peptide. We have synthesized seven polypeptides corresponding to each of the membrane-spanning α-helices in the native tertiary structure of bacteriorhodopsin, and we have characterized the structure of each individual synthetic peptide in reconstituted phospholipid vesicles. Six of these seven peptides are stably and irreversibly associated with reconstituted vesicles near neutral pH [see accompanying manuscript: Hunt et al. (1997)]; however, the peptide corresponding to the C-helix in the primary sequence of BR is only weakly associated with lipid vesicles and can be recovered at significant concentrations in a lipid-free supernatant following sedimentation of reconstituted vesicles. This observation led us to explore the solubility properties of the peptide in water in the absence of detergents, phospholipids, or chaotropic salts.

The purified and lyophilized synthetic peptide cannot be dissolved directly in an aqueous buffer, but it dissolves readily in a buffer containing 6 M urea. Following removal of all of the urea by extensive dialysis, the peptide can be recovered at concentrations greater than 5 mg/mL in a buffer containing only 20 mM NaCl and 5 mM $NaPO_4$ at pH 8.0. This solution can be passed through a 0.22 μm polycarbonate filter without a significant reduction in the concentration of the peptide.

We used gel filtration chromatography to characterize the aggregation state of the soluble BR-C peptide. The result of one such experiment is shown in Figure 2. The top trace shows the chromatographic profile observed when a sample of the peptide at pH 6.0 was concentrated to greater than 1 mg/mL and injected onto a TSK SW2000 column equilibrated in 200 mM NaCl, 50 mM $NaPO_4$ at pH 6.2. Five distinct features are observed in the chromatogram. (The final broad peak has a maximum after the fully-included volume; we believe that some of the peptide aggregates are large compared to the interstitial volume in the column bed, resulting in mechanical retardation of their migration.) Fractions were collected during this column run, and aliquots of some of these fractions were re-injected onto the column, as shown in the bottom three traces in Figure 2. The different hydrodynamic species in the concentrated stock solution are observed to be in equilibrium with the same species following

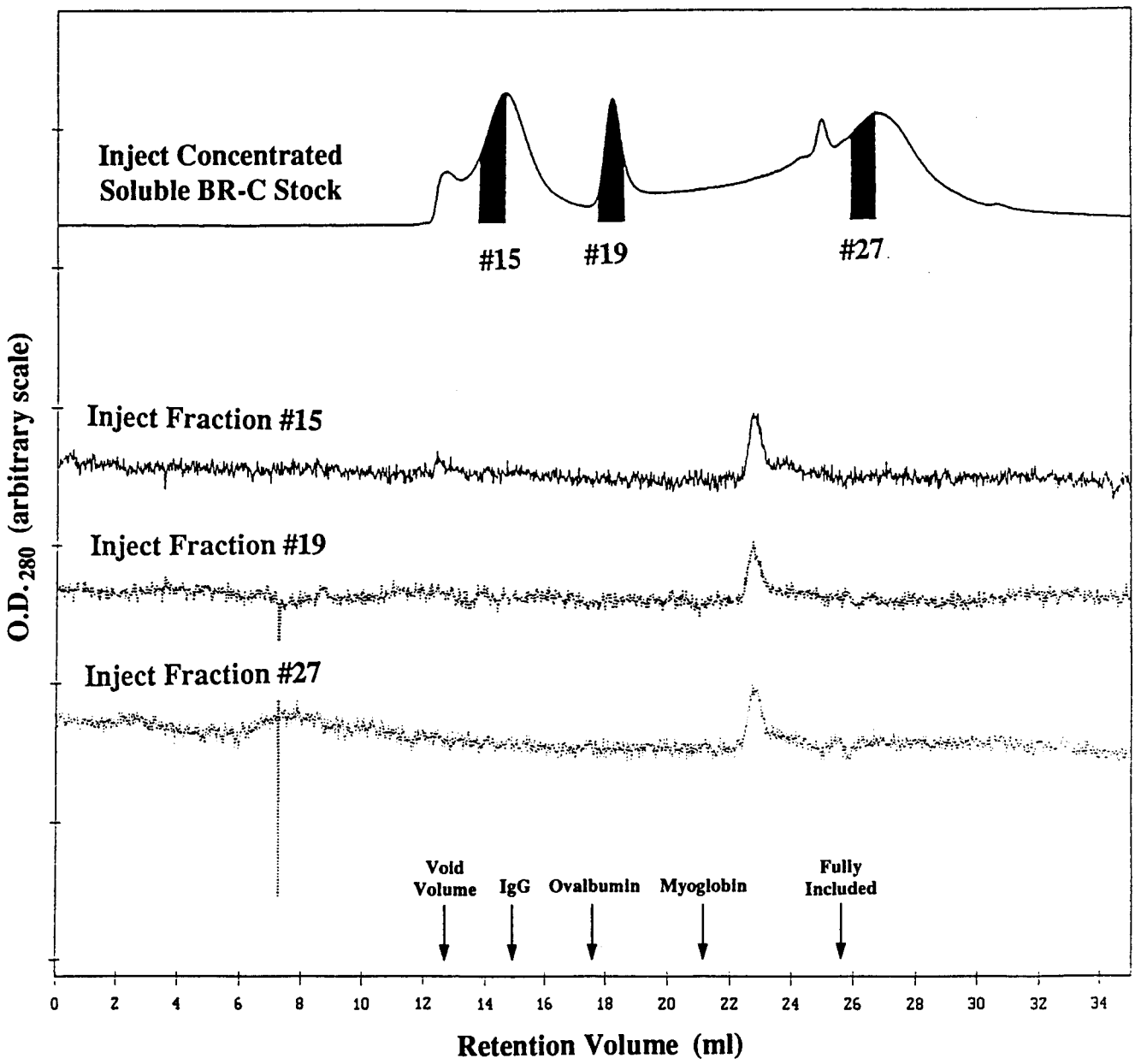

FIGURE 2: Gel filtration chromatography of the soluble BR-C peptide. An aliquot of the peptide at pH 6.0 was concentrated to greater than 1 mg/mL and injected onto a gel filtration column (top trace); a broad distribution of hydrodynamic species is observed. Fractions were collected from this initial column run and incubated overnight to allow re-equilibration of the aggregation state of the peptide following dilution during migration through the column. Aliquots from three of these fractions were re-injected onto the column (bottom three traces); the locations of these fractions in the original chromatogram are indicated schematically in the figure. The various peptide aggregates in the concentrated stock all appear to be in equilibrium with a single species with a relatively small hydrodynamic radius. The bold arrows at the bottom of the panel indicate the migration positions of five marker species on this gel filtration column; the molecular weights of the protein markers are 158 kDa (IgG), 44 kDa (ovalbumin), and 17 kDa (myoglobin).

dilution during the initial column run. The size of this species is small; it runs between markers for myoglobin (17 kDa) and the fully included volume (vitamin B12, 1.35 kDa) and has a nominal hydrodynamic radius of 16 Å (le Maire et al., 1989). We infer that this species has a well-defined aggregation state because the width at half-height of the corresponding chromatographic peak is identical to that observed for the individual globular marker proteins in the set used to calibrate the column.

Because CD spectroscopy shows that the peptide contains little regular secondary structure under these conditions, it could have an extended, nonglobular conformation (see Figure 4A below). Given this ambiguity, it is not possible to infer the aggregation state of the peptide from its hydrodynamic radius. The observed hydrodynamic radius of 16 Å is consistent with anything from a monomer of the peptide in an extended conformation to a trimer of the peptide in a compact, spherical conformation (Jorgensen & Møller, 1979; Flory, 1988).

Further chromatographic analyses show that the distribution of hydrodynamic species in the peptide stock solution is strongly dependent on the peptide concentration and on pH (data not shown). Stock solutions containing a high peptide concentration at pH 8 show predominantly a single peak at 18.4 mL on the gel filtration column corresponding to a nominal molecular weight of 36 kDa, as do stock solutions containing a lower peptide concentration at pH 6. An equivalent chromatographic peak can be observed in the center of the top trace in Figure 2 (*i.e.* the peak corresponding to fraction #19). The width at half-height of this peak is also identical to that of the individual globular marker proteins, suggesting that it is also a homogeneous species.

Thus, the soluble form of the BR-C peptide has a preferred oligomeric state in aqueous buffers. This oligomer is unlikely to be larger than an 9-mer of the BR-C peptide, which has a monomer molecular weight of 4.05 kDa.

Fluorescence emission spectroscopy can be used to study the oligomerization reaction of the soluble BR-C peptide. Following a 30-fold dilution of a stock solution of the peptide at pH 8 (to a final concentration of 12 μg/mL), there is a gradual change in the intrinsic fluorescence of the peptide (data not shown). The time evolution of the fluorescence is described by a single exponential with a half-time of 15 min, presumably corresponding to the rate constant for the dissociation of the dominant oligomer.

Binding of the Soluble BR-C Peptide to DMPC Vesicles at pH 7.8. The soluble form of the BR-C peptide binds spontaneously to phospholipid vesicles at pH 7.8. This binding can be monitored using fluorescence emission spectroscopy (Figure 3A,B). In this experiment, a dilute solution of the peptide ($\sim$12 μg/mL = 3 μM) was titrated with small unilamellar vesicles made from synthetic dimyristoylphosphatidylcholine (DMPC). The peptide was diluted from a concentrated stock solution and incubated overnight at the appropriate temperature for the binding experiment (35 °C) before adding phospholipid; a similar procedure was followed for all experiments involving the soluble BR-C peptide in order to assure equilibration of the aggregation state of the peptide. As shown in Figure 3A, the emission spectrum of the peptide has a maximum at 348 nm in the absence of phospholipid, consistent with both tryptophan side chains being exposed to an aqueous environment. Upon addition of 300 μg/mL of DMPC, there is a modest increase in the emission intensity and a blue-shift in the emission maximum to 342 nm. These changes are consistent with the movement of at least one of the tryptophan side chains into a more hydrophobic environment (McKnight et al., 1991; Chung et al., 1992).

The dependence of the binding reaction on the concentration of phospholipid is examined in Figure 3B. As an increasing amount of DMPC is added to the peptide solution, there is a progressive increase in fluorescence emission intensity. The corresponding spectra of the peptide show an isofluorescent point at 376 nm, consistent with a two-state binding reaction. It is not possible to quantitate the saturation phase of this reaction accurately using fluorescence spectroscopy because the light scattering produced by the DMPC vesicles eventually compromises the linear relationship between the quantum yield of the chromophore and the observed emission intensity. Thus, the nature of the binding reaction must be inferred from the functional form of the data at relatively low concentrations of DMPC.

We have chosen to analyze the binding isotherm using a stoichiometric binding equilibrium model rather than a partition model (White & Wimley, 1994) because the stoichiometric binding model affords a crude estimate of the size of the binding site based on saturation effects detectable at low lipid concentrations (*i.e.* high free peptide concentrations) when the affinity of the peptide for the bilayer is high, as it is for the interaction of the BR-C peptide with DMPC. A simple two-state model for the reaction postulates that there is a discrete binding site on the surface of the DMPC vesicle comprising n phospholipid molecules per peptide monomer (and that the aggregation state of the peptide does not change during binding), *i.e.*

$$\text{BR-C} + (n\text{DMPC}) \rightleftarrows (\text{BR-C}\cdot n\text{DMPC})$$

The phospholipid molecules comprising the binding site are assumed to be organized prior to interaction with the peptide so that the concentration of the site is given by ([DMPC]/n). In this case, the fraction of peptide bound at a given concentration of lipid can be described as

$$\phi_b([\text{DMPC}]) = 0.5[1 + (K_d/n[\text{BR-C}]) + ([\text{DMPC}]/n[\text{BR-C}]) - [[(K_d/n[\text{BR-C}]) + ([\text{DMPC}]/n[\text{BR-C}]) - 1]^2 + 4(K_d/n[\text{BR-C}])]^{1/2}]$$

In this equation, K_d represents the dissociation constant for the binding reaction expressed in terms of the molar concentration of phospholipid. [Note that this function reduces to the more familiar form, $\phi_b([\text{DMPC}]) = [\text{DMPC}]/(K_d + [\text{DMPC}])$ in the asymptotic limit as the term $(K_d/n[\text{BR-C}])$ grows large, *i.e.* as the peptide concentration becomes insignificant compared to the dissociation constant.] Using this nonlinear equation to fit the binding data in Figure 3B and allowing all parameters to vary freely, we derive optimum estimates of $K_d \approx 39$ μM (26 μg/mL) and $n \approx 9$ (continuous line in Figure 3B). However, we can obtain an adequate fit to the observed binding curve with n fixed at any value from 1 to 18, yielding estimates of K_d ranging from 11 to 69 μM.

The magnitude of the free energy released during the binding reaction (*i.e.* $\Delta G°$) can be calculated as $\Delta G° = RT \ln(K_d/n)$. Applying this formula to the optimum estimates of K_d and n given above yields an estimate of $\Delta G° = -7.5$ kcal/mol. This estimate of the binding energy should be reasonably accurate in spite of the relative imprecision in our estimates of K_d and n because of the logarithmic relationship between the free energy and the effective concentration of binding sites. Specifically, using fixed values of n ranging from 2 to 18 to analyze the observed binding data, our estimate of $\Delta G°$ varies only from -6.3 to -8.7 kcal/mol. Therefore, we feel confident that the standard free energy of the binding reaction falls within the range $\Delta G° = -7.5 \pm 1.4$ kcal/mol.

The secondary structure of the BR-C peptide in these samples can be monitored using circular dichroism spectroscopy (CD). Figure 4A shows the CD spectrum of a 10.4 μg/mL solution of the soluble BR-C peptide at pH 7.6 in the absence of phospholipid. There is minimal ellipticity between 210 and 230 nm, indicating the presence of little regular secondary structure in the peptide free in solution. Figure 4A also shows the CD spectrum of this solution following the addition of small unilamellar DMPC vesicles to a final concentration of 250 μg/mL. Although there is a small increase in the magnitude of the molar ellipticity of the peptide at 222 nm, the α-helix content of the peptide population is still small based on both the magnitude and the shape of the CD spectrum (Johnson, 1988).

In the absence of regular secondary structure, the hydrogen bonding capacity of the peptide backbone cannot be systematically fulfilled by intramolecular contacts, making it unlikely that it is buried in the hydrophobic region of the bilayer (Engelman & Steitz, 1981). Since the BR-C peptide contains little α-helical structure when bound to DMPC bilayers at neutral pH, we believe that it must be bound to the membrane in a peripheral location under these conditions.

The pH-Dependent Transition in DMPC Vesicles. Upon acidification of the solution, large changes are observed in

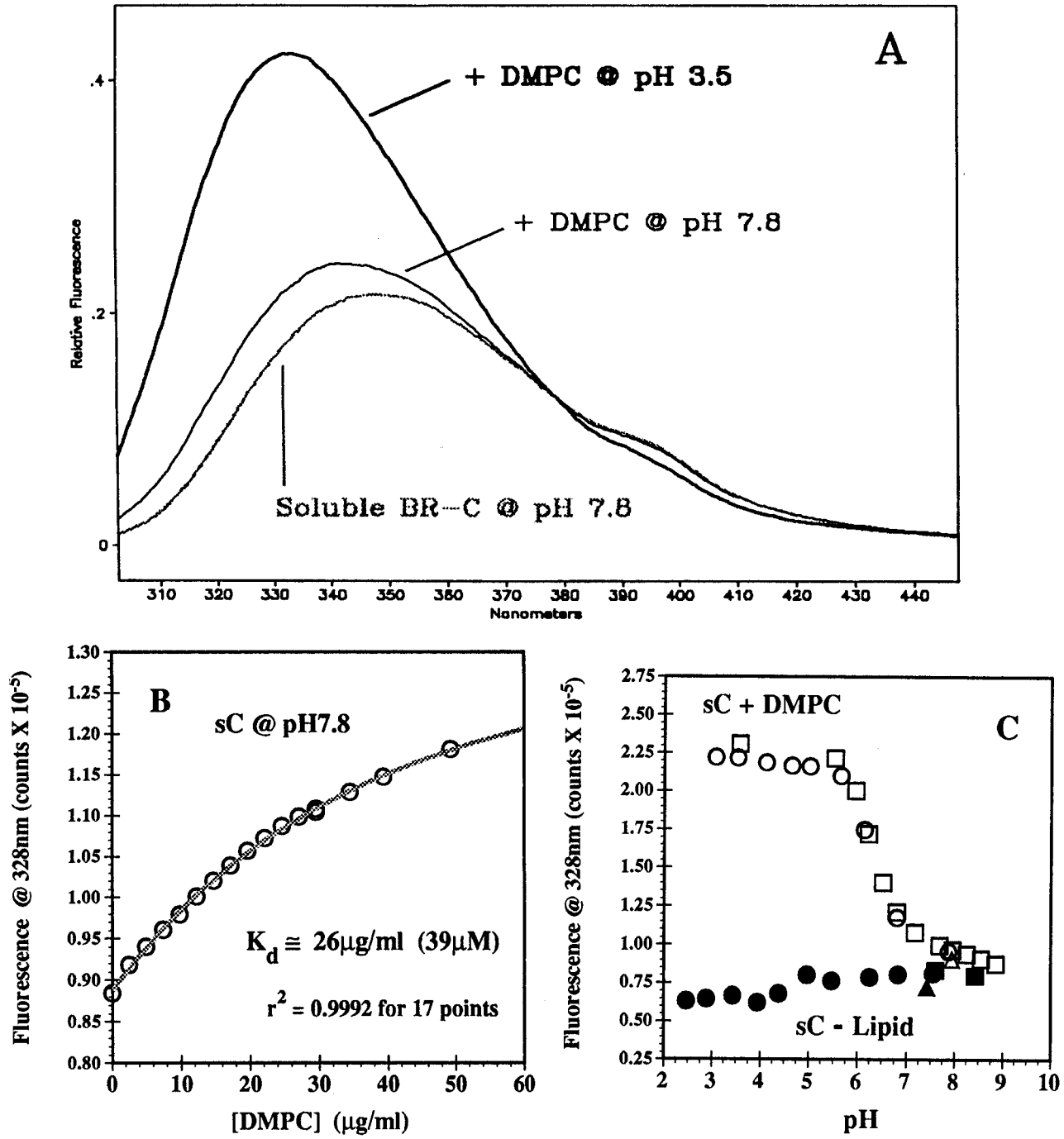

FIGURE 3: Fluorescence spectroscopy of the soluble BR-C peptide (sC) and its pH-dependent interactions with DMPC vesicles at 35 °C. The intrinsic fluorescence of the peptide was monitored using an excitation wavelength of 280 nm. (A) Fluorescence emission spectra of a 12 μg/mL (3 μM) solution of the BR-C peptide at pH 7.8 before (gray line) and after (thin black line) the addition of DMPC vesicles at 300 μg/mL; the thick black line shows the fluorescence emission spectrum of the same peptide solution in the presence of DMPC vesicles after titration to pH 3.5. (B) Binding curve at pH 7.8 showing the fluorescence emission intensity of the BR-C peptide as a function of the concentration of added DMPC. The gray line represents the optimized fit to these data using the two-state binding equation specified in the body of the text; this curve corresponds to a dissociation constant of 26 μg/mL (39 μM) and a binding site of 9 DMPC molecules per peptide monomer. The emission intensity was monitored at 328 nm for this experiment and for the experiments shown in the next panel. (C) pH titration of the BR-C peptide in the presence of DMPC vesicles at 300 μg/mL (open symbols) and in the absence of phospholipid (closed symbols) as monitored using the intrinsic fluorescence of the peptide. There is evidence of a discrete transition with a pK_a of approximately 6 which results in a major increase in the fluorescence quantum yield of the peptide. The transition is fully reversible as evidenced by the reproducibility of the measurements during repeated titrations up (□, △) and down (○) in pH. There is no evidence of a pH-dependent transition in the environment of the peptide fluorophores in the absence of phospholipid.

both the fluorescence emission spectrum and the CD spectrum of the BR-C peptide in the presence of DMPC vesicles at 250 μg/mL. Figure 3A shows fluorescence emission spectra acquired at pH 7.8 and 3.5. A major increase is observed in the fluorescence quantum yield at acidic pH as well as a blue-shift in the emission maximum from 342 to 333 nm. Subtracting the spectrum at pH 7.8 from the spectrum at pH 3.5 reveals a very strong peak with a maximum at 326 nm (data not shown); there is a 2.5-fold increase in the fluorescence emission intensity at this wavelength. These changes are consistent with a tryptophan side chain on the peptide moving into the hydrophobic core of the lipid bilayer (McKnight et al., 1991; Chung et al., 1992). There are two tryptophan residues in the synthetic

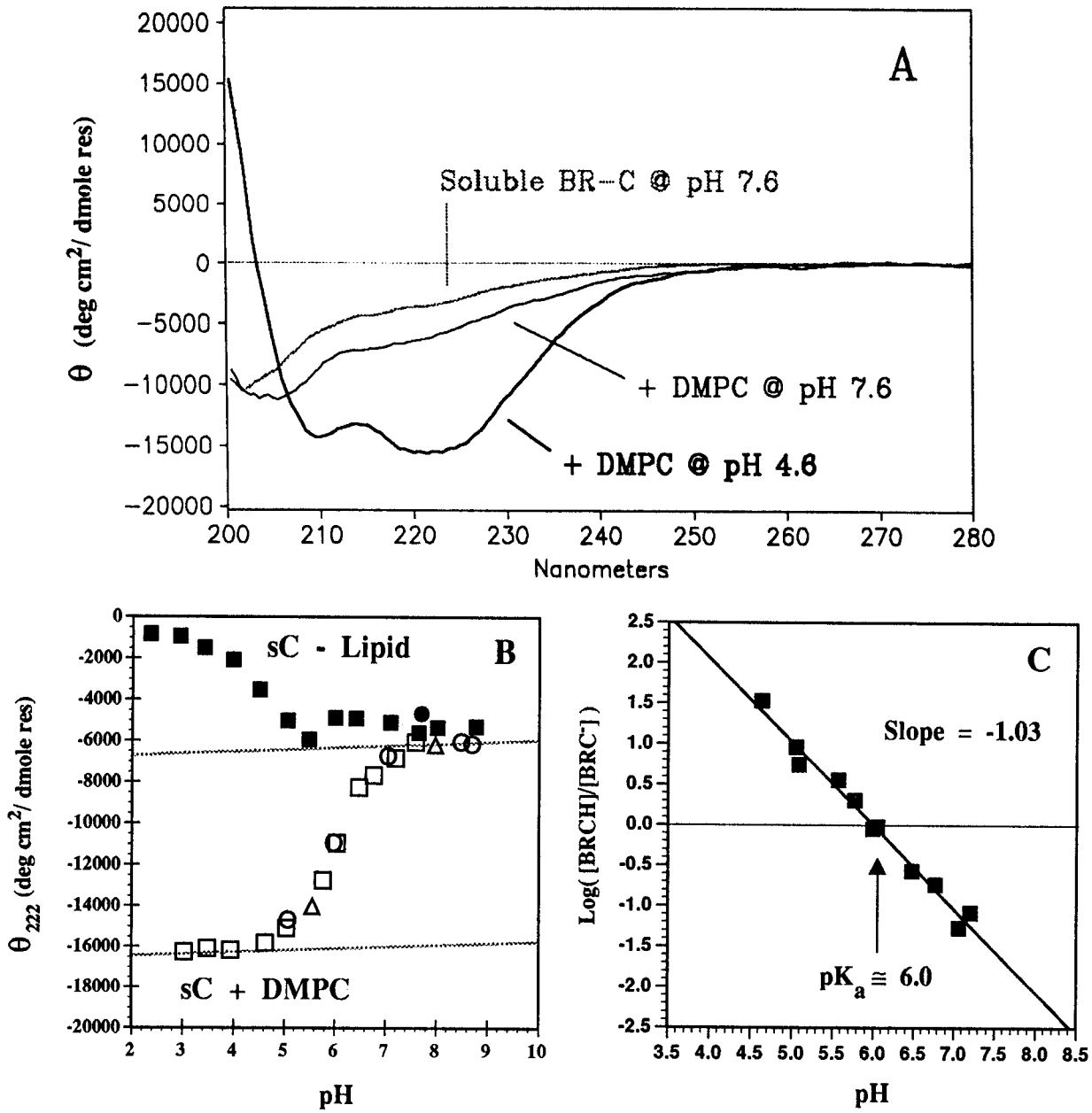

FIGURE 4: Circular dichroism spectroscopy of the soluble BR-C peptide and its pH-dependent interactions with DMPC vesicles at 35 °C. (A) CD spectra of a 12 μg/mL (3 μM) solution of the BR-C peptide at pH 7.8 before (gray line) and after (thin black line) addition of DMPC vesicles at 250 μg/mL; the thick black line shows the CD spectrum of the same peptide solution in the presence of DMPC vesicles after titration to pH 4.6. (B) pH titration of the BR-C peptide in the presence of DMPC vesicles at 250 μg/mL (open symbols) and in the absence of phospholipid (closed symbols) as monitored by the mean residue ellipticity of the peptide at 222 nm. The peptide adopts a largely α-helical conformation at low pH, but only in the presence of phospholipid. The transition in the presence of phospholipid is fully reversible as evidenced by the reproducibility of the measurements during repeated titrations down (□, △) and up (○) in pH. The two continuous lines represent the inferred baselines for the CD of the protonated and de-protonated forms of the peptide in DMPC and are used to calculate the data shown in panel C. (C) Log−log plot of the equilibrium constant for the transition in DMPC *versus* hydrogen ion concentration. The slope of this line (−1.03) corresponds to the number of protons involved in the transition; the pK_a is calculated to be 6.03 by adding a factor of log(1 + (K_d/[DMPC])) to 5.99, which is the intercept of the line on the pH axis (see the section on "Quantitative Analysis of pH Titration Data" in the Experimental Procedures).

BR-C peptide (Figure 1) at positions 9 and 15 (corresponding to trp-80 and trp-86 in the native sequence of BR).

The pH dependence of this change in the fluorescence emission intensity of the peptide is plotted in Figure 3C. A discrete transition with a pK_a of approximately 6.0 is observed when the titration is performed in the presence of DMPC vesicles. However, there is no evidence of a pH-dependent transition in the environment of the peptide in the absence of the vesicles, showing that the transition is strictly phospholipid-dependent.

CD spectroscopy reveals that the BR-C peptide undergoes a pH-dependent conformational transition in the presence of DMPC vesicles that parallels the transition observed using fluorescence spectroscopy. Figure 4A shows CD spectra acquired at pH 7.6 and 4.6. The BR-C peptide adopts a largely α-helical conformation at low pH in the presence of phospholipid. The pH dependence of this conformational change is plotted explicitly in Figure 4B. Again, a discrete transition with a pK_a of approximately 6.0 is observed when the titration is performed in the presence of DMPC vesicles. (Consistent with a two-state transition, the spectra acquired in the course of this titration show an iso-dichroic point at 206.5 nm.) From the shape of the titration curve, the number of protons involved in the conformational transition can be

determined. Specifically, the value of the ellipticity at a given pH can be used to infer the ratio of the concentration of the low pH form of the peptide to the concentration of the high pH form of the peptide. The logarithm of this ratio is plotted against pH in Figure 4C. The data yield a straight line with a slope of −1.03 indicating that the net titration of one proton per cooperative unit is responsible for the helix−coil transition. The simplest explanation for this result is that the protonation of a single amino acid side chain is responsible for inducing the conformational change. We calculate that the pK_a of the proton involved in the helix−coil transition is 6.03 based on the intercept of the line on the pH axis (see Experimental Procedures).

In a control titration conducted in the absence of phospholipid (Figure 4B), no increase in α-helix content is observed at low pH. (Under these conditions, the magnitude of the molar ellipticity at 222 nm decreases at pH values below 5.0, and a faint, grainy precipitate is observed in the peptide solution.) Therefore, the pH-dependent conformational transition of the BR-C peptide is absolutely dependent on the presence of the DMPC vesicles.

From these data, it appears that the titration of one proton equivalent on the BR-C peptide is coupled to a transition to an α-helical conformation. This conformational transition is coincident with the movement of a tryptophan residue into a buried position in the lipid bilayer, as would be expected during the insertion of the peptide into the membrane in the form of a transbilayer α-helix. There are two aspartic acid residues (asp-85 and asp-96) in the membrane-embedded region of the C-helix in the native structure of BR based on the analysis of Henderson and co-workers using high-resolution electron crystallography (Grigorieff et al., 1996). We believe that it is likely that the protonation of one of these carboxylic acid side chains controls the insertion of the helix into the membrane. The anomalous pK_a of 6.0 could result from coupling of the protonation of the side chain to another energetically favorable process. We propose that the protonation of either asp-85 or asp-96 is energetically coupled to the insertion of the BR-C peptide into the membrane in the form of a transbilayer α-helix.

The observed pK_a of the transition can be used to infer the free energy of the insertion reaction based on consideration of the following formal thermodynamic cycle:

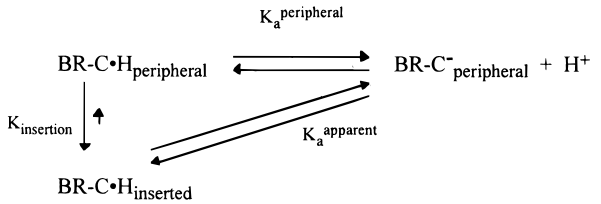

In this scheme, $K_a^{peripheral}$ represents the equilibrium constant for the protonation of the relevant carboxylate group in the peripherally bound conformation of the peptide, and $K_{insertion}$ represents the equilibrium constant for the membrane insertion of the protonated form of the peptide. Given this scheme, the free energy of the insertion reaction is described by the following equation:

$$\Delta G_{insertion} = -RT \ln(K_{insertion}) = -RT \ln(10)(pK_a^{apparent} - pK_a^{peripheral})$$

If $K_{insertion} \gg 1$, the transition from the peripherally-bound, deprotonated state to the membrane-inserted, protonated state will proceed without significant population of the peripherally-bound, protonated state, and the empirically observed titration will correspond directly to $K_a^{apparent}$ in the thermodynamic cycle defined above. Assuming that $pK_a^{peripheral} \cong 4.0$ (*i.e.* a standard value for the pK_a of a carboxylate group in an aqueous environment), we infer that the transbilayer configuration of the protonated BR-C peptide is favored compared to the most stable peripheral configuration by $\Delta G_{insertion} \cong -2.9$ kcal/mol. The corresponding value of $K_{insertion} \cong 120 \gg 1$ validates the assumption used in analyzing the pH titration data. Nonetheless, the quantitative estimate of the free energy of insertion must be considered approximate because of the potential inaccuracy in the assumed value of $pK_a^{peripheral}$ (Dempsey, 1990).

To study the reversibility of the pH-dependent conformational transition, each sample was titrated three times, with the direction of each successive titration (in terms of pH) opposite to that of the previous titration (Figures 3C and 4B). These experiments show that the conformational transition of the BR-C peptide in the presence of DMPC vesicles is fully reversible.

Polarized FTIR Studies of DMPC Multilayers. The experiments described above suggest that the BR-C peptide may spontaneously insert into the membrane in the form of a transbilayer α-helix at low pH. However, these experiments do not rule out the possibility that the low pH form of the peptide is an α-helix lying parallel to surface of the membrane which positions a tryptophan side chain at the interface of the hydrophobic region of the bilayer. In order for an α-helix to span the bilayer, its axis must be nearly perpendicular to the plane of the bilayer. Therefore, in order to test our hypothesis that the low pH form of the BR-C helix in the presence of DMPC corresponds to a transbilayer α-helix, we sought to establish the orientation of the BR-C helix relative to the plane of the phospholipid bilayer. Polarized Fourier transform infrared spectroscopy (FTIR) of macroscopically ordered protein/phospholipid multilayers (Rothschild & Clark, 1979) provides a convenient assay of protein orientation in membranes.

Like most phospholipids, DMPC adopts a multilamellar phase at high relative humidity in the absence of bulk water (Büldt et al., 1978). When vesicles in aqueous solution are dried down onto a solid planar support, they produce a macroscopically ordered multilamellar phase with the individual membrane bilayers oriented parallel to the plane of the support (Büldt et al., 1978). This multilamellar phase has been exploited in many biophysical studies of phospholipids and membrane proteins because the orientation of molecular structures relative to the plane of the membrane can be inferred from measuring their orientation relative to the macroscopic sample plane. In particular, polarized FTIR of multilamellar films has been used to characterize the orientation of protein secondary structure relative to the plane of the bilayer for a wide variety of integral membrane proteins (Nabedryk & Breton, 1981; Nabedryk et al., 1988; Earnest et al., 1990; Rothschild & Clark, 1979).

We produced macroscopically ordered multilayers (Clark et al., 1980) from DMPC vesicles containing the BR-C peptide. Polarized FTIR spectra of a sample deposited at pH 5.3 are shown in Figure 5A. For these measurements, the surface normal to the sample plane of the multilamellar film was tilted 45° relative to the incident infrared beam. The two lower traces in Figure 5A show absolute infrared absorbance spectra which were acquired with the incident

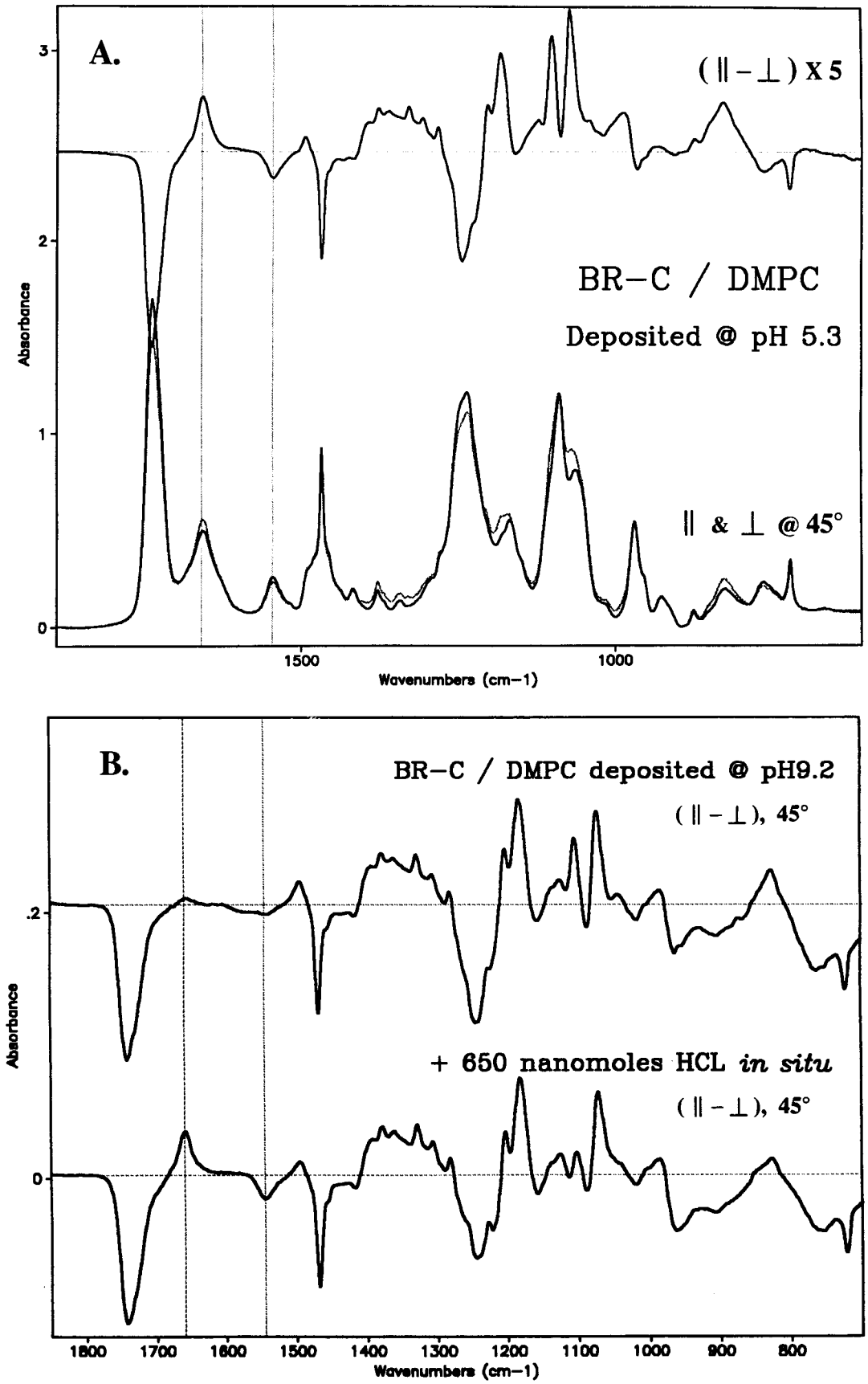

FIGURE 5: Polarized FTIR spectroscopy of macroscopically ordered DMPC multilayers containing the BR-C peptide. (A) Spectra of multilayers deposited at pH 5.3 and measured with the surface normal to the sample plane tilted 45° relative to the incident beam. The two lower traces represent absolute absorbance spectra acquired with parallel or perpendicular polarization of the beam relative to the optical plane of incidence. The upper trace represents the difference between these two spectra magnified by a factor of 5. The thin vertical lines indicate the positions of the protein amide I absorbance at 1658 cm^{-1} and the protein amide II absorbance at 1545 cm^{-1}. (B) The sample from Figure 5A was resuspended, titrated to pH 9.2, and re-deposited for further FTIR studies. The upper trace in this panel is a polarized difference spectrum ($\| - \perp$ polarization) of this sample at 45° tilt. The lower trace is a polarized difference spectrum of the same film at 45° tilt after acidification *in situ* with 650 nmol of HCl (see Experimental Procedures). Dichroism plots for a set of protein and lipid absorbances in these samples are presented in Figure S1 in the Supporting Information for this paper.

beam polarized either parallel or perpendicular to the optical plane of incidence. The top trace is a magnified view (5×) of the difference between these two spectra; a signal is observed in this "dichroism spectrum" only if the molecular oscillator giving rise to an infrared absorbance has a net orientation relative to the macroscopic sample plane. Given the format in which the data is plotted in Figure 5, a transition dipole moment with an out-of-plane orientation will produce a positive peak while a transition dipole moment with an in-plane orientation will produce a negative peak (Rothschild & Clark, 1979). Most of the peaks in this spectrum are attributable to lipid vibrations (Casal & Mantsch, 1984), *e.g.* the carbonyl stretching mode at 1739 cm^{-1}, the methylene scissoring mode at 1468 cm^{-1}, the phosphate antisymmetric stretching mode at 1243 cm^{-1}, and the ester C−O stretching mode at 1183 cm^{-1}. However, two peaks are attributable to vibrational modes of the peptide bonds in the protein backbone (Miyazawa, 1958, 1960); the amide I band at 1658 cm^{-1} represents a stretching mode of the carbonyl bond while the amide II band at 1545 cm^{-1} represents a coupled C−N stretching and N−H rocking mode. In the BR-C/DMPC multilayers, these two modes have a different net orientation relative to the plane of the membrane, *i.e.* the amide I mode is primarily perpendicular to the plane of the membrane while the amide II mode is primarily parallel to the plane of the membrane. This is precisely the relative orientation of these vibrational modes anticipated for a transbilayer α-helix (Rothschild & Clark, 1979).

The most reliable quantitation of the orientation of the molecular oscillators in these samples is derived from analysis of a "tilt series" in which infrared spectra are acquired with the sample tilted at a number of different angles relative to the incident beam (Rothschild & Clark, 1979). The dichroic ratio for a given peak (*i.e.* the ratio of the absorbance measured using the two orthogonal polarizations of the incident beam) is plotted as a function of $\sin^2(\alpha)$, where α represents the angle of inclination of the surface normal of the sample relative to the incident beam. This plot should produce a straight line, and the slope of the line is related to the order parameter for the transition dipole moment of the molecular oscillator. Moreover, the linearity of the plot is an important control on the validity of the dichroism data. Tilt series data for a set of protein and lipid absorbances in the BR-C/DMPC sample deposited at pH 5.3 are presented in Figure S1A in the Supporting Information. These plots verify our assumptions about the structure and orientation of the phospholipid bilayers in the sample and allow us to quantitate the orientation of the protein α-helices relative to the membrane.

The protein amide II peak yields the most accurate estimate of protein orientation because of the absence of other strong absorbances in the spectral region from 1500 to 1600 cm^{-1}. The magnitude of the dichroism in this BR-C peptide sample corresponds to an order parameter of −0.23 for the amide II transition dipole moment. The meaning of this figure can be interpreted by comparison to equivalent samples of native BR which are characterized by an amide II order parameter of −0.24 (Rothschild & Clark, 1979; Earnest et al., 1990). Thus, the ensemble average of the orientation of the peptide bonds in BR multilayers is very similar to that observed in the BR-C multilayers. Essentially all of the α-helices in native BR have a transbilayer orientation (Grigorieff et al., 1996), so, by analogy, the α-helices in the BR-C sample must be oriented roughly perpendicular to the plane of the membrane. Quantitatively, the dichroism data are consistent with every BR-C peptide forming an α-helix 20 residues long with its axis tilted approximately 15° from perpendicular to the plane of the bilayer.

In order to establish whether the pH-dependent conformational properties of the BR-C peptide are equivalent in phospholipid multilayers and in vesicles in solution, we resuspended the sample that produced the spectra shown in Figure 5A, titrated it to pH 9.2 using NaOH, and re-deposited it for further spectroscopic studies. The upper trace in Figure 5B shows that the dichroism of the protein peaks has been mostly eliminated even though the dichroism of the lipid peaks is unchanged. Therefore, the protein has become disordered relative to the phospholipid bilayer which remains oriented. Absolute absorbance spectra of this sample (data not shown) show changes which are consistent with a transition in the conformation of the BR-C peptide, *i.e.* a broadening of the amide I and amide II band envelopes as well as a 3 cm^{-1} shift to lower frequency in both of these peaks relative to the spectra of the same sample deposited at pH 5.3.

Finally, we investigated whether the BR-C peptide could insert into the bilayer *in situ* in the multilamellar film. Thus, the sample which had been deposited at pH 9.2 was acidified by adding 650 nmol of HCl to the surface of the film in a 10 μL drop. As shown in the bottom trace in Figure 5B, the protein dichroism returned after this treatment. Tilt series data for this multilamellar film before and after acidification are shown in Figure S1B in the Supporting Information. The dichroism of the lipid peaks is not changed by acidification of the film, indicating that the molecular structure of the phospholipid multilayers is conserved; however, the dichroism of both of the protein peaks increases dramatically, returning to values equivalent to those observed in this sample when it was deposited originally at pH 5.3. Therefore, the α-helix has spontaneously re-inserted into the bilayer in response to acidic pH.

Based on the results of these FTIR experiments in conjunction with the results of the fluorescence experiments and the CD experiments performed on vesicles in solution, we conclude that the BR-C peptide spontaneously inserts into DMPC membranes as a transbilayer α-helix in response to reduced pH.

Comparison of the pH-Dependent Transition in Halo-Lipid Vesicles. We have also investigated the dependence of the conformational properties of the BR-C peptide on the chemical composition of the phospholipid bilayer. DMPC does not occur in the native lipid environment in *H. salinarium* (Kates et al., 1982). The native lipids contain exclusively diphytanoyl acyl chains (*i.e.* 3*R*,7*R*,11*R*,15-tetramethylhexadecyl) which are connected to the phospholipid head group by ether linkages. Moreover these lipids do not contain phosphatidylcholine head groups; instead, they contain phosphatidylglycerol (∼5%), phosphatidylglycerophosphate (∼70%), phosphatidylglycerosulfate (∼5%), and glycolipid sulfate (∼20%) (Kates et al., 1982). To explore the influence of these differences in lipid composition, we have characterized the pH-dependent conformational properties of the BR-C peptide in membranes made from a polar lipid extract from *H. salinarium* (*Halo*-lipids). We have performed a complete set of spectroscopic experiments in this phospholipid environment analogous to the experiments described above. As shown in Table 1, the BR-C peptide displays essentially identical conformational be-

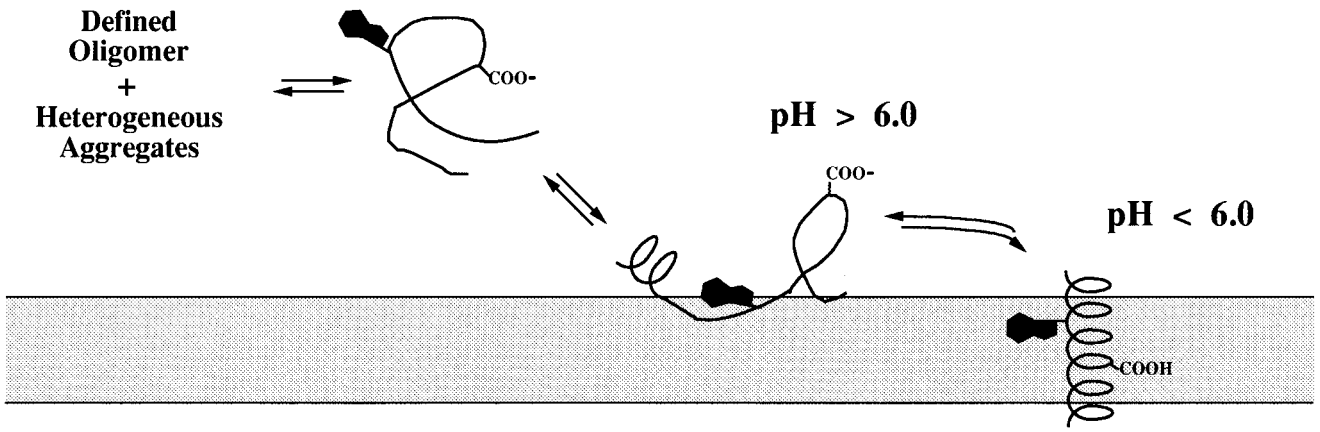

FIGURE 6: Schematic diagram of the observed conformational properties of the BR-C peptide.

havior in the two radically different phospholipid environments.

At pH 7.8, the BR-C peptide binds reversibly to *Halo*-lipid vesicles, although the dissociation constant is substantially higher than that observed for DMPC vesicles (K_d = 380 μM *vs* 39 μM for DMPC). The high dissociation constant for *Halo*-lipid vesicles may be attributable to electrostatic effects. The peptide should carry a net charge of −5 at neutral pH while the *Halo*-lipids are characterized by a high proportion of anionic head groups (Kates et al., 1982); because the binding assay is conducted at very low ionic strength (5 mM $NaPO_4$, 20 mM NaCl), electrostatic repulsion between the peptide and the membrane would be expected to elevate the observed K_d. However, the pH-dependent conformational properties of the membrane-associated BR-C peptide are essentially identical in the two phospholipid environments. In both cases, a discrete conformational transition with a pK_a of approximately 6 in vesicles in solution is associated with an acid-induced transition from a disordered state to an α-helix directed perpendicular to the plane of the membrane in oriented phospholipid multilayers.

DISCUSSION

A schematic summary of the observed conformational properties of the BR-C peptide is presented in Figure 6. We have not established which acidic group on the BR-C peptide is responsible for gating the insertion of the α-helix into the membrane. We assume that this residue is either asp-85 or asp-96, *i.e.* one of the two acidic groups in the membrane-spanning region of this helix in the native structure of BR (Grigorieff et al., 1996; Khorana et al., 1979). Based on the pH dependence of the transition, we believe that only one of these two residues is protonated during the insertion reaction, indicating that the other is either protonated in the peripheral conformation of the peptide or deprotonated in the transbilayer conformation of the peptide. If asp-96 is present as a carboxylate in the transmembrane conformation, we assume that it is located in the polar headgroup region of the bilayer. However, if asp-85 is present as a carboxylate in the transmembrane conformation, it could form a tightly bonded ion pair with arg-82 in the hydrophobic region of the bilayer (Engelman & Steitz, 1981). In this configuration, the protonation state of both asp-85 and asp-96 would be the same as in the ground state of native bacteriorhodopsin as determined by FTIR difference spectroscopy (Braiman et al., 1988; Bousché et al., 1991; Gerwert et al., 1989; Rothschild & Sonar, 1995). Further experimentation will be required to establish the actual protonation state of acidic residues in the transbilayer conformation of the BR-C peptide.

On the basis of the observed conformational behavior of the BR-C peptide, we believe that spontaneous and uncatalyzed insertion of a transbilayer α-helix into a phospholipid membrane can occur on a fast enough time scale to play a role in the biosynthesis of integral membrane proteins. We have not characterized the kinetics of the insertion reaction in detail, but we have performed pH jump experiments on the peptide in DMPC vesicles at 35 °C. Two exponentials are required to fit the time course of the change in fluorescence emission intensity following a jump from pH 7.8 to 5.8 (data not shown). One exponential is characterized by a half-time of approximately 3 s and accounts for 70% of the magnitude of the transition while the other is characterized by a half-time of approximately 28 s. We do not know whether there are two populations which insert at different rates or whether there is a single population which proceeds to the final state through a kinetic intermediate. However, following a pH jump in the opposite direction, the conformational transition is completed by the time we can get a reliable measurement of the fluorescence emission intensity (approximately 4 s), indicating that the aspartic acid residue in the hydrophobic region of the bilayer can sense the external proton concentration very rapidly. Most importantly, the observed insertion rate is fast enough that the spontaneous insertion process could play a role in integral membrane protein biosynthesis.

Cellular chaperones (Hartl, 1996; Landry & Gierasch, 1994) and translocases (Blobel, 1980; Nicchitta et al., 1991; Wickner, 1994; den Blaauwen & Driessen, 1996) are likely to be intimately involved in the assembly of integral membrane proteins *in vivo*. For instance, molecular chaperones may be involved in delivering hydrophobic nascent chains to the surface of the membrane (Kumamoto, 1991; Ulbrandt et al., 1997). Furthermore, it seems very improbable that spontaneous insertion could account for the transmembrane translocation of the large polar loops found between some adjacent transbilayer α-helices (Blobel, 1980; Manoil & Beckwith, 1986; von Heijne, 1994b); cellular translocases must be involved in catalyzing insertion of transbilayer α-helices into the membrane under these circumstances. However, uncatalyzed insertion may play a role in integral membrane protein biosynthesis, particularly when there is a relatively short loop between adjacent transbilayer helices (Abrams et al., 1991; Slatin et al., 1994; von Heijne,

1994a,b). Physiological experiments have been conducted in *E. coli* which suggest that the mechanism of membrane protein integration differs depending on the length of the protein sequence which is translocated through the membrane (Andersson & von Heijne, 1993; Manoil & Beckwith, 1986; McGovern & Beckwith, 1991; Cao et al., 1995); translocation of a large protein domain requires active participation by the SecA component of the bacterial secretory apparatus while translocation of a short protein sequence (<60 residues) may not (von Heijne, 1994a; Traxler & Murphy, 1996). The spontaneous insertion process described in this paper could explain the molecular mechanism of this "Sec-independent" membrane integration phenomenon observed *in vivo* in bacteria (von Heijne, 1994a).

We believe that the BR-C peptide represents a system in which the kinetics and thermodynamics of α-helix insertion into phospholipid membranes can be studied quantitatively and systematically in order to provide a foundation for understanding the physical chemistry of integral membrane protein assembly. The effect of variations in the sequence of the peptide on the kinetics of insertion can be monitored conveniently using fluorescence spectroscopy. For example, experiments of this type could be used to quantitate the effect of electrostatic charge in the flanking sequences on the activation energy for the insertion of the helix into the bilayer. Moreover, the sequence dependence of the free energy of insertion can be monitored by measuring changes in the pK_a of the transition. Experiments of this type could be used to refine theoretical schemes for the analysis of integral membrane protein structure and folding. In the case of the BR-C helix, the algorithm of Goldman, Engelman, and Steitz (Engelman et al., 1986) predicted a free energy change of −19 kcal/mol for the insertion the helix into a phospholipid membrane at neutral pH. We have determined that the experimental value for the BR-C peptide is closer to −6.1 kcal/mol in DMPC membranes, representing a discrepancy of +13 kcal/mol in the observed *vs* predicted values of $\Delta G_{insertion}$. However, there is a peripheral conformation of the peptide which is 1.4 kcal/mol lower in free energy than the integral conformation at neutral pH.

Bechinger (1996) has also reported a pH-dependent equilibration between a membrane-inserted and peripheral conformation for a model transbilayer α-helix containing histidine in its membrane-spanning region (although this experimental system did not allow evaluation of the kinetics of the membrane insertion reaction beyond establishing them as slow on the time scale of ^{15}N nuclear magnetic resonance spectroscopy). In this case, titration to higher pH leads to deprotonation and charge-neutralization of histidine and gates membrane insertion of the peptide. Furthermore, Ren et al. (1997) have reported that changes in the hydrophobic thickness of the bilayer can gate transitions between membrane-inserted and peripheral conformations for a set of model transbilayer α-helices of varying hydrophobic length. It has previously been suggested that peripherally membrane-associated protein structures could play a kinetic role in the pathway of membrane protein insertion (Jacobs & White, 1989; White & Wimley, 1996; Kleinschmidt & Tamm, 1996). However, the possibility of a stable membrane-associated peripheral conformation has not been considered explicitly in most of the theoretical analyses of integral membrane protein structure or the associated structure-prediction schemes (von Heijne, 1980; Kyte & Doolittle, 1982; Engelman et al., 1986); the experimental observations of such a peripheral conformation represents a complication in terms of the predictive accuracy of these schemes since they generally assume that a transbilayer α-helical conformation is the only stable membrane-associated conformation for a hydrophobic peptide sequence of adequate length.

Our estimate of $\Delta G_{insertion}$ must be considered preliminary since we are not certain of the oligomeric state of the BR-C peptide either free in solution or integrated into the bilayer; oligomeric interactions in either state would influence the observed free energy of insertion, as would stable tertiary structure in the soluble form of the peptide monomer. However, experimental studies on the membrane-insertion of the M13 coat protein have indicated that the magnitude of $\Delta G_{insertion}$ for its transbilayer α-helix is at most −15 kcal/mol (Soekarjo et al., 1996) compared to a predicted value of −27 kcal/mol (Engelman et al., 1986). And studies of the membrane insertion of a 20 residue polyalanine helix have indicated that its free energy of insertion is at most −5 kcal/mol compared to a predicted value of −20 kcal/mol (Moll & Thompson, 1994). Therefore, there is a similar quantitative discrepancy greater than +12 kcal/mol in the observed *vs* predicted values of $\Delta G_{insertion}$ for three different transbilayer α-helices.

Engelman et al. (1986) calculated that $\Delta G_{insertion} \leq -16$ kcal/mol for all of the experimentally observed transbilayer helices; this figure greatly exceeds the magnitude that would be required to stably anchor a helix in the membrane, leading these authors to conclude that their algorithm might overestimate the magnitude of the free energy of insertion. The quantitative discrepancy observed for the three transbilayer helices could be attributable to the formation of compact tertiary structure by the peptides when they are in the soluble state (Moll & Thompson, 1994; Leto & Holloway, 1979), which would result in partial burial of their hydrophobic side chains; in this case, the reference state that was assumed in the calculations would not be appropriate because it assumed complete exposure of the side chains to the aqueous environment. However, the quantitative discrepancy between the observed *vs* predicted values of $\Delta G_{insertion}$ could also be attributable to the polarity of the polypeptide backbone (Roseman, 1988; Wimley & White, 1996), a factor that was not considered in the theoretical treatment of the insertion process (Engelman et al., 1986). Roseman (1988) has determined that the free energy of transferring a single hydrogen-bonded C═O···N−H group from water to hydrocarbon is approximately +0.55 kcal/mol, which would correspond to approximately +9 kcal/mol for an α-helix 20 residues in length. This number is similar in magnitude to the discrepancy in the observed *vs* predicted free energy of insertion for the transbilayer α-helices for which this quantity has been measured.

We also suggest that the spontaneous insertion of transbilayer α-helices may present an approach to moving chemical reagents through the permeability barrier of biological membranes. Insertion of the BR-C helix into the membrane involves passing one terminus of the peptide through the hydrophobic core of the bilayer. The amino terminus of our synthetic peptide has 8 residues outside of the region predicted to be in the transbilayer helix; this sequence will carry one positive charge and one negative charge at neutral pH. The carboxy terminus has 6 residues which will carry 4 negative charges at neutral pH. We have not characterized the relative rate at which the two termini of our synthetic peptide pass through the bilayer. However,

both ends of the peptide contain reasonably hydrophilic sequences which carry formal electrostatic charge, and it is unlikely that either the octamer at the amino terminus or the hexamer at the carboxy terminus would exhibit significant permeability through biological membranes as an isolated polypeptide. Nonetheless, at least one of these segments is efficiently translocated through the bilayer during the insertion of the BR-C helix. By extension, it might be possible to facilitate the passage of a membrane-impermeant reagent through the bilayer by attaching it to the appropriate end of the BR-C helix. There will be limits to the size and polarity of reagents that can be attached to the peptide without inhibiting the insertion of the helix into the membrane, but straightforward experiments can be designed to test these limits using the convenient spectroscopic properties of the BR-C peptide system.

The relatively rapid time-scale and the reversibility of the pH-dependent conformational transition of the BR-C peptide raise the possibility that spontaneous insertion of transbilayer α-helices could play a role in integral membrane protein function (Nishiyama et al., 1996). For example, acidic pH activates membrane penetration for a wide variety of protein toxins (Neville & Hudson, 1986); pH-dependent insertion of transbilayer α-helices could play a role in this process. Moreover, pH regulation of a membrane transport process could be achieved by moving a transbilayer α-helix which forms an indispensable part of a transport enzyme into or out of the membrane in response to changes in pH (Bechinger, 1996). Activation of an ion channel could be accomplished using an analogous mechanism, *i.e.* by inserting into the membrane one of the helices lining the conducting pore of the channel; voltage gating of the channel could be controlled simply by varying the number of acidic and basic residues at the terminus of the helix which is translocated though the membrane during activation (Aggarwal & MacKinnon, 1996). A related phenomenon has been observed in studies on the renal Na,K-ATPase antiporter. Following limited proteolysis of vesicles containing this protein, a polypeptide fragment comprising a pair of transbilayer α-helices is rapidly released into the supernatant (Lutsenko et al., 1995); a glutamic acid residue that has been identified as part of the binding site for the K^+ ion is located in the transmembrane region of one of these helices (Arguello & Kaplan, 1994), while a pair of aspartic acid residues are located in the transmembrane region of the other. The helix containing the glutamatic acid residue that contributes to the K^+ ion binding site is believed to move relative to the plane of the membrane during the reaction cycle of the transporter (Lutsenko et al., 1995); the results presented in this paper raise the possibility that the entire helix could insert into and retract from the membrane in the course of the transport reaction. Obviously, there are other molecular mechanisms that could be used in all of these systems to achieve equivalent results. Nonetheless, our observations with the BR-C peptide indicate that the reversible insertion and ejection of transbilayer α-helices can occur on a fast enough time scale to play an active role in physiological processes.

Finally, we note that asp-96 in the C-helix is normally protonated in the photochemical ground state of BR, consistent with its position in hydrophobic interior of the protein (Braiman et al., 1988; Grigorieff et al., 1996). However, during the M → N transition of the BR photocycle, a protein conformational change occurs which is correlated with the deprotonation of asp-96 (Bousché et al., 1991; Braiman et al., 1991). After this conformational change, asp-96 must have access either directly or indirectly to the cytoplasmic medium since it subsequently reprotonates from that side of the membrane. This reprotonation is accompanied by a reversal of the conformational change that occurred during the M → N transition (Bousché et al., 1992). Although the structural details of this conformational change including the role of the C-helix have yet to be elucidated (Steinhoff et al., 1994), the fundamental steps in the BR photocycle/proton-transport cycle involve a coupling between the ionization state of asp-96 and the protein structure which modulates the access of an external proton to asp-96. Therefore, both the photocycle of BR and the spontaneous membrane-insertion of the isolated BR-C helix involve a coupling between protein structure and the protonation state of an aspartic acid residue in the transmembrane region of the C-helix.

ACKNOWLEDGMENT

We acknowledge productive discussions with Anne Metcalf, Joe Kim, and Krishna Kalghatgi as well as generous assistance from Olaf Bousché, Jim Elliot, Myron Crawford, and Agnes "Nessie" Stewart. We thank John Flanagan, Mark Lemmon, Mischa Machius, and Paula Booth for critical evaluation of the manuscript.

SUPPORTING INFORMATION AVAILABLE

Dichroism plots quantitating the variation of the dichroic ratio as a function of sample tilt angle for a set of protein and lipid absorbances in the samples shown in Figure 5 (2 pages). See any current masthead page for ordering and access information.

REFERENCES

Abrams, C. K., Jakes, K. S., Finkelstein, A., & Slatin, S. L. (1991) *J. Gen. Physiol. 98*, 77.
Aggarwal, S. K., & MacKinnon, R. (1996) *Neuron 16*, 1169.
Anderson, D. J., Mostov, K. E., & Blobel, G. (1983) *Proc. Natl. Acad. Sci. U.S.A. 80*, 7249.
Andersson, H., & von Heijne, G. (1993) *EMBO J. 12*, 683.
Arguello, J. M., & Kaplan, J. H. (1994) *J. Biol. Chem. 269*, 6892.
Audigier, Y., Friedlander, M., & Blobel, G. (1987) *Proc. Natl. Acad. Sci. U.S.A. 84*, 5783.
Bassford, P., Beckwith, J., Ito, K., Kumamoto, C., Mizushima, S., Oliver, D., Randall, L., Silhavy, T., Tai, P. C., & Wickner, B. (1991) *Cell 65*, 367.
Bayle, D., Weeks, D., & Sachs, G. (1995) *J. Biol. Chem. 270*, 25678.
Bechinger, B. (1996) *J. Mol. Biol. 263*, 768.
Ben-Efraim, I., Bach, D., & Shai, Y. (1993) *Biochemistry 32*, 2371.
Ben-Efraim, I., Strahilevitz, J., Bach, D., & Shai, Y. (1994) *Biochemistry 33*, 6966.
Blobel, G. (1980) *Proc. Natl. Acad. Sci. U.S.A. 77*, 1496.
Booth, P. J., Farooq, A., & Flitsch, S. L. (1996) *Biochemistry 35*, 5902.
Bousché, O., Braiman, M., He, Y. W., Marti, T., Khorana, H. G., & Rothschild, K. J. (1991) *J. Biol. Chem. 266*, 11063.
Bousché, O., Sonar, S., Krebs, M. P., Khorana, H. G., & Rothschild, K. J. (1992) *Photochem. Photobiol. 56*, 1085.
Braiman, M. S., Mogi, T., Marti, T., Stern, L. J., Khorana, H. G., & Rothschild, K. J. (1988) *Biochemistry 27*, 8516.
Braiman, M. S., Bousché, O., & Rothschild, K. J. (1991) *Proc. Natl. Acad. Sci. U.S.A. 88*, 2388.
Büldt, G., Gally, H. U., Seelig, A., Seelig, J., & Zaccaï, G. (1978) *Nature 271*, 182.
Cao, G., Kuhn, A., & Dalbey, R. E. (1995) *EMBO J. 14*, 866.
Casal, H. L., & Mantsch, H. H. (1984) *Biochim. Biophys. Acta 779*, 381.
Chung, L. A., & Thompson, T. E. (1996) *Biochemistry 35*, 11343.

Chung, L. A., Lear, J. D., & DeGrado, W. F. (1992) *Biochemistry 31*, 6608.
Clark, N. A., Rothschild, K. J., Luippold, D. A., & Simon, B. A. (1980) *Biophys. J. 31*, 65.
de Kruijff, B. (1994) *FEBS Lett. 346*, 78.
Dempsey, C. E. (1990) *Biochim. Biophys. Acta 1031*, 143.
den Blaauwen, T., & Driessen, A. J. (1996) *Arch. Microbiol. 165*, 1.
Denzer, A. J., Nabholz, C. E., & Spiess, M. (1995) *EMBO J. 14*, 6311.
Earnest, T. N., Roepe, P. D., Braiman, M. S., Gillespie, J., & Rothschild, K. J. (1986) *Biochemistry 25*, 7793.
Earnest, T. N., Herzfeld, J., & Rothschild, K. J. (1990) *Biophys. J. 58*, 1539.
Engelman, D. M., & Steitz, T. A. (1981) *Cell 23*, 411.
Engelman, D. M., Steitz, T. A., & Goldman, A. (1986) *Annu. Rev. Biophys. Biophys. Chem. 15*, 321.
Enoch, H. G., Fleming, P. J., & Strittmatter, P. (1979) *J. Biol. Chem. 254*, 6483.
Flory, P. J. (1988) in *Statistical Mechanics of Chain Molecules*, Oxford University Press, New York.
Geller, B. L., & Wickner, W. (1985) *J. Biol. Chem. 260*, 13281.
Gerwert, K., Hess, B., Soppa, J., & Oesterhelt, D. (1989) *Proc. Natl. Acad. Sci. U.S.A. 86*, 4943.
Goormaghtigh, E., De Meutter, J., Szoka, F., Cabiaux, V., Parente, R. A., & Ruysschaert, J. M. (1991) *Eur. J. Biochem. 195*, 421.
Grigorieff, N., Ceska, T. A., Downing, K. H., Baldwin, J. M., & Henderson, R. (1996) *J. Mol. Biol. 259*, 393.
Hartl, F. U. (1996) *Nature 381*, 571.
Henderson, R., Baldwin, J. M., Ceska, T. A., Zemlin, F., Beckmann, E., & Downing, K. H. (1990) *J. Mol. Biol. 213*, 899.
Hunt, J. F., Earnest, T. N., Bousché, O., Kalghatgi, K., Reilly, K., Horváth, C., Rothschild, K. J., & Engelman, D. M. (1997) *Biochemistry 36*, 15156−15176.
Jacobs, R. E., & White, S. H. (1989) *Biochemistry 28*, 3421.
Johnson, W. C., Jr. (1988) *Annu. Rev. Biophys. Biophys. Chem. 17*, 145.
Jorgensen, K. E., & Møller, J. V. (1979) *Am. J. Physiol. 236*, F103.
Kates, M., Kushwaha, S. C., & Sprott, G. D. (1982) *Methods Enzymol. 88*, 98.
Khorana, H. G. (1988) *J. Biol. Chem. 263*, 7439.
Khorana, H. G., Gerber, G. E., Herlihy, W. C., Gray, C. P., Anderegg, R. J., Nihei, K., & Biemann, K. (1979) *Proc. Natl. Acad. Sci. U.S.A. 76*, 5046.
Kleinschmidt, J. H., & Tamm, L. K. (1996) *Biochemistry 35*, 12993.
Kumamoto, C. A. (1991) *Mol. Microbiol. 5*, 19.
Kyte, J., & Doolittle, R. F. (1982) *J. Mol. Biol. 157*, 105.
Landry, S. J., & Gierasch, L. M. (1994) *Annu. Rev. Biophys. Biomol. Struct. 23*, 645.
le Maire, M., Aggerbeck, L. P., Monteilhet, C., Andersen, J. P., & Møller, J. V. (1986) *Anal. Biochem. 154*, 525.
le Maire, M., Ghazi, A., Martin, M., & Brochard, F. (1989) *J. Biochem. 106*, 814.
Leto, T. L., & Holloway, P. W. (1979) *J. Biol. Chem. 254*, 5015.
Lutsenko, S., Anderko, R., & Kaplan, J. H. (1995) *Proc. Natl. Acad. Sci. U.S.A. 92*, 7936.
Manoil, C., & Beckwith, J. (1986) *Science 233*, 1403.
McGovern, K., & Beckwith, J. (1991) *J. Biol. Chem. 266*, 20870.
McKnight, C. J., Rafalski, M., & Gierasch, L. M. (1991) *Biochemistry 30*, 6241.
Miczak, A., Kaberdin, V. R., Wei, C. L., & Lin-Chao, S. (1996) *Proc. Natl. Acad. Sci. U.S.A. 93*, 3865.
Miyazawa, T. (1958) *J. Chem. Phys. 29*, 611.
Miyazawa, T. (1960) *J. Chem. Phys. 32*, 1647.
Moll, T. S., & Thompson, T. E. (1994) *Biochemistry 33*, 15469.
Mueckler, M., & Lodish, H. F. (1986) *Cell 44*, 629.
Nabedryk, E., & Breton, J. (1981) *Biochim. Biophys. Acta 635*, 515.
Nabedryk, E., Garavito, R. M., & Breton, J. (1988) *Biophys. J. 53*, 671.
Neville, D. M., Jr., & Hudson, T. H. (1986) *Annu. Rev. Biochem. 55*, 195.
Nicchitta, C., Migliaccio, G., & Blobel, G. (1991) *Methods Cell Biol. 34*, 263.
Nishiyama, K., Suzuki, T., & Tokuda, H. (1996) *Cell 85*, 71.
Oesterhelt, D., & Stoeckenius, W. (1971) *Nature, New Biol. 233*, 149.
Peled, H., & Shai, Y. (1994) *Biochemistry 33*, 7211.
Peled-Zehavi, H., Arkin, I. T., Engelman, D. M., & Shai, Y. (1996) *Biochemistry 35*, 6828.
Popot, J. L., Gerchman, S. E., & Engelman, D. M. (1987) *J. Mol. Biol. 198*, 655.
Reddy, A. P., Tallon, M. A., Becker, J. M., & Naider, F. (1994) *Biopolymers 34*, 679.
Ren, J., Lew, S., Wang, Z., & London, E. (1997) *Biochemistry 36*, 10213.
Roseman, M. A. (1988) *J. Mol. Biol. 201*, 621.
Rothschild, K. J., & Clark, N. A. (1979) *Biophys. J. 25*, 473.
Rothschild, K. J., & Sonar, S. (1995) in *CRC Handbook of Organic Photochemistry and Photobiology* (Horspool, W. M., & Song, P.-S., Eds.) pp 1521−1544, CRC Press, Inc., London.
Savitzky, A., & Golay, M. J. E. (1964) *Anal. Chem. 36*, 1627.
Silver, P., Watts, C., & Wickner, W. (1981) *Cell 25*, 341.
Slatin, S. L., Qiu, X. Q., Jakes, K. S., & Finkelstein, A. (1994) *Nature 371*, 158.
Soekarjo, M., Eisenhawer, M., Kuhn, A., & Vogel, H. (1996) *Biochemistry 35*, 1232.
Steinhoff, H. J., Mollaaghababa, R., Altenbach, C., Hideg, K., Krebs, M., Khorana, H. G., & Hubbell, W. L. (1994) *Science 266*, 105.
Surrey, T., Schmid, A., & Jahnig, F. (1996) *Biochemistry 35*, 2283.
Traxler, B., & Murphy, C. (1996) *J. Biol. Chem. 271*, 12394.
Ulbrandt, N. D., Newitt, J. A., & Bernstein, H. D. (1997) *Cell 88*, 187.
von Heijne, G. (1980) *Eur. J. Biochem. 103*, 431.
von Heijne, G. (1989) *Nature 341*, 456.
von Heijne, G. (1994a) *FEBS Lett. 346*, 69.
von Heijne, G. (1994b) *Annu. Rev. Biophys. Biomol. Struct. 23*, 167.
von Heijne, G., & Blomberg, C. (1979) *Eur. J. Biochem. 97*, 175.
von Heijne, G., & Gavel, Y. (1988) *Eur. J. Biochem. 174*, 671.
Watts, C., Silver, P., & Wickner, W. (1981) *Cell 25*, 347.
White, S. H., & Wimley, W. C. (1996) *Curr. Opin. Struct. Biol. 4*, 79.
Whitley, P., Zander, T., Ehrmann, M., Haardt, M., Bremer, E., & von Heijne, G. (1994) *EMBO J. 13*, 4653.
Wickner, W. (1980) *Science 210*, 861.
Wickner, W. T. (1994) *Science 266*, 1197.
Wimley, W. C., & White, S. H. (1996) *Nat. Struct. Biol. 3*, 842.
Wolfe, P. B., Rice, M., & Wickner, W. (1985) *J. Biol. Chem. 260*, 1836.

BI970147B